This is a preprint of: "Topological classification of some SD Hamiltonian systems", Ting Chen, Jaume Llibre, *Differ. Equ. Dyn. Syst.*, 2023.
DOI: [10.1007/s12591-023-00637-y]

TOPOLOGICAL CLASSIFICATION OF SOME SD HAMILTONIAN SYSTEMS

TING CHEN[1] AND JAUME LLIBRE[2,*]

Abstract. In this paper we classify the phase portraits in the Poincaré disk of the Smooth and Discontinuous (SD) Hamiltonian system with the rational Hamiltonian function $H(x,y) = y^2/2 + P(x)/Q(x,y)$, where $P(x) = a$, ax, ax^2 and $Q(x,y) = Ax^2 + By^2 + C$.

1. Introduction and statement of the main results

In this paper we deal with the Hamiltonian system

$$\dot{x} = H_y(x,y), \qquad \dot{y} = H_x(x,y), \tag{1}$$

with a rational potential

$$H(x,y) = \frac{y^2}{2} + V(x,y) = \frac{y^2}{2} + \frac{P(x)}{Q(x,y)}, \tag{2}$$

where $P(x) = a$, ax, ax^2 and $Q(x,y) = Ax^2 + By^2 + C$ with $aAB \neq 0$. The system associated to the Hamiltonian function (2) has the form

$$\dot{x} = y - \frac{P(x)\partial_y(Q(x,y))}{Q^2(x,y)}, \qquad \dot{y} = \frac{\partial_x(Q(x,y))P(x) - \partial_x(P(x))Q(x,y)}{Q^2(x,y)}, \tag{3}$$

where $\partial_x(\cdot)$ and $\partial_y(\cdot)$ indicate the derivatives of the polynomials with respect to x and y respectively, and the dot denotes derivative with respect to the real variable t, which is called the *time*. We denote by the set $L = \{(x,y)|Q(x,y) = 0\}$ the points where the Hamiltonian system (3) is not defined. To be more precise system (3) is a *Smooth* and *Discontinuous* Hamiltonian system (SD Hamiltonian system), the smooth dynamic behavior appears when the set L is empty, while the discontinuous dynamics occurs when L is not empty. By the rescaling of the time

$$\frac{dt}{d\tau} = Q^2(x,y), \tag{4}$$

the SD Hamiltonian system (3) becomes the polynomial differential system

$$\begin{aligned} x' =& yQ^2(x,y) - P(x,y)\partial_y(Q(x,y)), \\ y' =& \partial_x(Q(x,y))P(x) - \partial_x(P(x))Q(x,y), \end{aligned} \tag{5}$$

where x' and y' denote derivatives of x and y with respect to τ respectively. The new system (5) is not Hamiltonian in general, but it has a first integral of motion. For analyzing the phase portrait of the SD Hamiltonian system (3), we can study

2010 *Mathematics Subject Classification.* Primary: 34C07, 34C08.
Key words and phrases. SD Hamiltonian system, equilibrium point, infinity, separatrix, phase portrait.

the phase portrait associated to the polynomial differential system (5) and after we eliminate the set L.

The classification of the global phase portraits of the planar polynomial differential systems in Poincaré disk started with the work of Vulpe [25] and Schlomiuk [24]. Artés and Llibre [2] classified the phase portraits of all quadratic Hamiltonian systems in the Poincaré disk. Guillamon et al. [16] studied the phase portraits of the separable Hamiltonian systems whose Hamiltonian function is $H(x, y) = F(x) + G(y)$. The works [10, 12, 18] classified the global phase portraits of all linear type centers of polynomial Hamiltonian systems having cubic or quartic homogeneous terms. The phase portraits of cubic Liénard systems with global parameters in the cases of two and three equilibria have been studied in [5, 6]. For some other interesting results related with phase portraits of polynomial differential systems see [3, 4, 7, 8, 9, 11, 13, 15, 17]. Recently, the authors of [19] presented the phase portraits of the quadratic polynomial systems with a rational first integral of degree 3. Martínez and Vidal [21] provided the phase portraits of the rational Hamiltonian systems with some potential of the form $V(x) = P(x)/Q(x)$. Our main results are the following ones.

Theorem 1.1. *The phase portraits in the Poincaré disk of the SD Hamiltonian systems (3) with* $H_1(x, y) = \frac{y^2}{2} + \frac{a}{Ax^2+By^2+C}$ *and* $aAB \neq 0$ *are topologically equivalent to some of the phase portraits from 1.1 to 1.18 of Figure 1.*

Theorem 1.2. *The phase portraits in the Poincaré disk of the SD Hamiltonian systems (3) with* $H_2(x, y) = \frac{y^2}{2} + \frac{ax}{Ax^2+By^2+C}$ *and* $aAB \neq 0$ *are topologically equivalent to some of the phase portraits from 1.19 to 1.26 of Figures 1 and 2.*

Theorem 1.3. *The phase portraits in the Poincaré disk of the SD Hamiltonian systems (3) with* $H_3(x, y) = \frac{y^2}{2} + \frac{ax^2}{Ax^2+By^2+C}$ *and* $aAB \neq 0$ *are topologically equivalent to some of the phase portraits from 1.1, 1.8, 1.11, 1.12 and 1.27 to 1.36 of Figures 1 and 2.*

In the phase portraits of the above results the set L is indicated by a dash line or a dash curve "$---$" in the Poincaré disk. And the dash line "$\cdots$" in the phase portraits denotes that it is filled of equilibria. On the other hand, a small circle in the phase portrait denotes an equilibrium point of the polynomial system (5), but no an equilibrium point of the SD Hamiltonian system (3), and we called it a *virtual equilibrium point* or a *virtual singular point*. We denote by S and R the number of *separatrices* and of *canonical regions* of a phase portrait in the Poincaré disk, respectively. It is known that the separatrices of a polynomial differential system in the Poincaré disk are all the infinite orbits, all the finite equilibrium points, the separatrices of the hyperbolic sectors of the finite and infinite equilibrium points, and the limit cycles. Here we do not have to consider the limit cycles of system (3) because the existence of a first integral prevents the existence of limit cycles. For more details about separatrices and canonical regions see [14].

The remaining sections are organized as follows. In Section 2 we include some basic results that we shall use later on. In Section 3-5 we classify the phase portraits in the Poincaré disk for the SD Hamiltonian systems (3), in other words we prove Theorems 1.1–1.3.

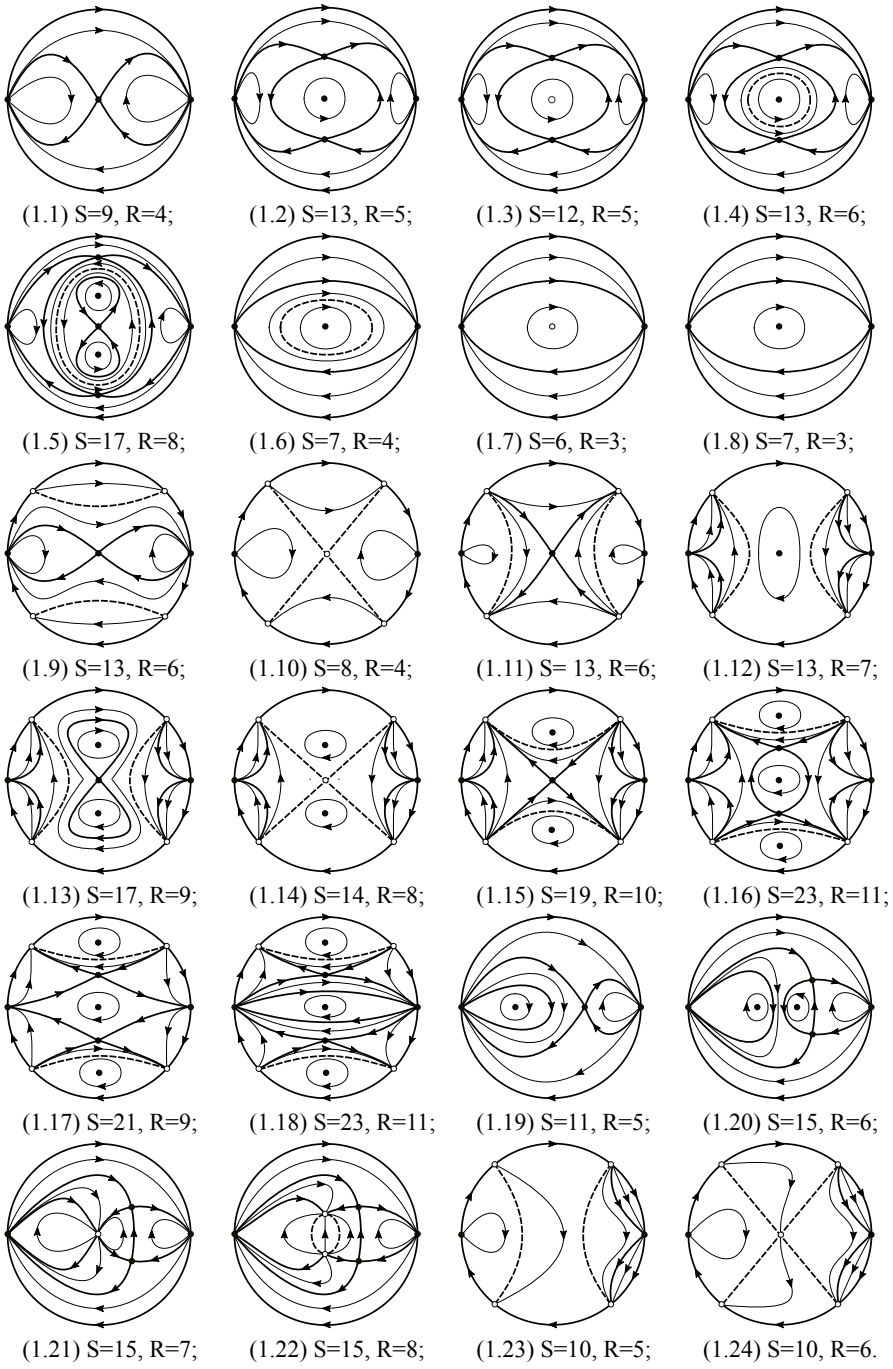

FIGURE 1. Topological phase portraits of cases 1.1-1.24 of Theorems 1.1 and 1.2.

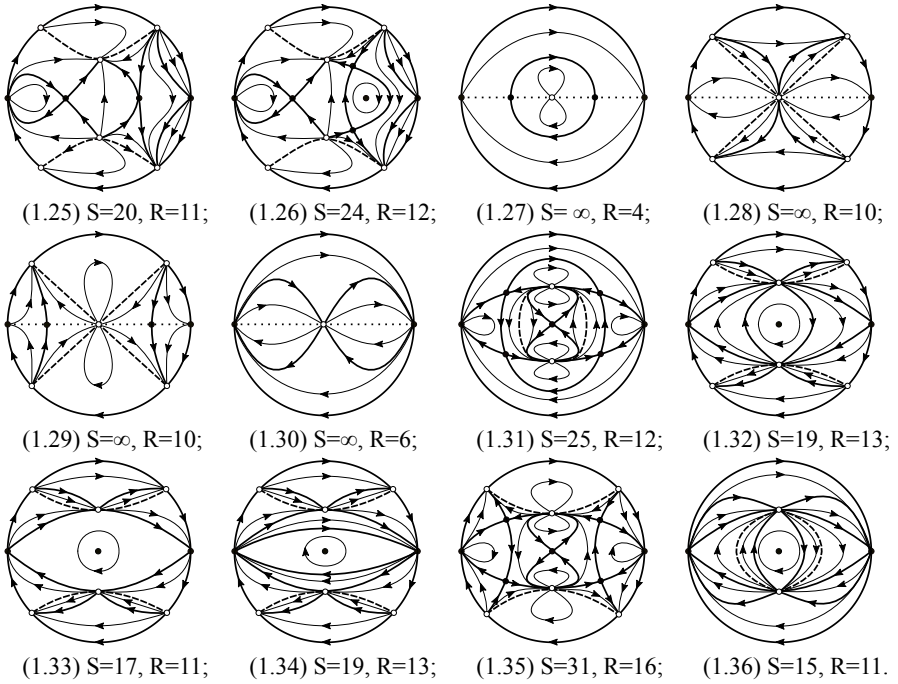

FIGURE 2. Topological phase portraits of cases 1.25-1.36 of Theorems 1.2 and 1.3.

2. Basic results

In this section we recall the method for analyzing the local phase portraits of finite and infinite equilibrium points of a polynomial vector field in the Poincaré disk.

2.1. **Poincaré compactification.** We identify the plane $\mathbb{R}^2$ as the plane in $\mathbb{R}^3$ defined by the points $\mathbf{s} = (s_1, s_2, s_3) = (x_1, x_2, 1)$. Let $P(\mathbb{R}^2)$ be the set of all polynomial vector fields $\mathcal{X}$ in $\mathbb{R}^2$ of the form

$$(\dot{x_1}, \dot{x_2}) = (X(x_1, x_2), Y(x_1, x_2)), \tag{6}$$

where X and Y are real polynomials in the variables x_1 and x_2 of degree d_1 and d_2, respectively. Taking $d = \max\{d_1, d_2\}$. The vector field $p(\mathcal{X})$ is called the *Poincaré compactification* of the vector field $\mathcal{X}$, for more details see Chapter 5 of [14].

Let $\mathbb{S}^2 = \{\mathbf{s} \in \mathbb{R}^3 : s_1^2 + s_2^2 + s_3^2 = 1\}$ be the *Poincaré sphere*. The plane $\mathbb{R}^2$ is tangent to $\mathbb{S}^2$ at the point $(0, 0, 1)$. By projecting each point $x \in \mathbb{R}^2$ onto two points of the Poincaré sphere we can study the phase portrait of $\mathcal{X}$ on the plane $\mathbb{R}^2$. This projection is given by the intersection of the straight line through x and the origin of $\mathbb{R}^3$ with the sphere $\mathbb{S}^2$. It provides a vector field $\mathcal{X}'$ formed by two copies of $\mathcal{X}$, one on the open northern hemisphere and the other on the open southern hemisphere. We denote by $\mathbb{S}^1 = \{\mathbf{s} \in \mathbb{S}^2 : \ s_3 = 0\}$ the equator of $\mathbb{S}^2$ which corresponds to the infinity of $\mathbb{R}^2$. In order to extend the vector field $\mathcal{X}'$ on $\mathbb{S}^2 \setminus \mathbb{S}^1$ to a vector field $p(\mathcal{X})$ on the whole sphere $\mathbb{S}^2$ we multiply the vector field $\mathcal{X}'$ by x_3^d.

In summary, there are two symmetric copies of $\mathcal{X}$ on $\mathbb{S}^2 \setminus \mathbb{S}^1$ and the behavior of $p(\mathcal{X})$ near $\mathbb{S}^1$ corresponds the behavior of $\mathcal{X}$ near the infinity. To draw the phase portraits of $p(\mathcal{X})$ we will consider the orthogonal projection $(x_1, x_2, x_3) \to (x_1, x_2)$ of the closed northern hemisphere of $\mathbb{S}^2$ centered at the origin of coordinates into the close disk $\mathbb{D}^2 = \{(x_1, x_2) \in \mathbb{R}^2 : x_1^2 + x_2^2 \leq 1\}$, called the Poincaré disk.

On the Poincaré sphere $\mathbb{S}^2$ we use the following six local charts to do the calculations, which are given by $U_i = \{\mathbf{s} \in \mathbb{S}^2 : \ s_i > 0\}$ and $V_i = \{\mathbf{s} \in \mathbb{S}^2 : \ s_i < 0\}$, for $i = 1, 2, 3$, with the corresponding diffeomorphisms

$$\varphi_i : \ U_i \to \mathbb{R}^2, \qquad \psi_i : \ V_i \to \mathbb{R}^2, \tag{7}$$

defined by $\varphi_i(\mathbf{s}) = -\psi_i(\mathbf{s}) = (s_m/s_i, s_n/s_i) = (u, v)$ for $m < n$ and $m, n \neq i$. Thus (u, v) will play different roles in the distinct local charts. The expression of the vector field $p(\mathcal{X})$ are

$$(\dot{u}, \dot{v}) = (v^d \left[Y\left(\frac{1}{v}, \frac{u}{v}\right) - uX\left(\frac{1}{v}, \frac{u}{v}\right) \right], -v^{d+1} X\left(\frac{1}{v}, \frac{u}{v}\right)) \qquad \text{in } U_1, \tag{8}$$

$$(\dot{u}, \dot{v}) = (v^d \left[X\left(\frac{u}{v}, \frac{1}{v}\right) - uY\left(\frac{u}{v}, \frac{1}{v}\right) \right], -v^{d+1} Y\left(\frac{u}{v}, \frac{1}{v}\right)) \qquad \text{in } U_2, \tag{9}$$

$$(\dot{u}, \dot{v}) = (X(u, v), Y(u, v)) \qquad \text{in } U_3. \tag{10}$$

The expressions of $p(\mathcal{X})$ in V_i is the same as in U_i multiplied by $(-1)^{d-1}$ for $i = 1, 2, 3$. Thus it is enough to study its Poincaré compactification restricted to the northern hemisphere plus $\mathbb{S}^1$ for studying the vector field $\mathcal{X}$.

The equilibrium points of $p(\mathcal{X})$ in the Poincaré disk lying on $\mathbb{S}^1$ are the *infinite equilibrium points* of the corresponding vector field $\mathcal{X}$. The equilibria of $p(\mathcal{X})$ in the interior of the Poincaré disk, i.e. on $\mathbb{S}^2 \setminus \mathbb{S}^1$, are the *finite equilibrium points*. So it is sufficient to study the equilibrium points at $U_1|_{v=0}$ and at the origin of U_2 for studying the infinite equilibrium points of $\mathcal{X}$, and use U_3 for computing the finite equilibrium points. Note that if $\mathbf{s} \in \mathbb{S}^1$ is an infinite equilibrium point, then $-\mathbf{s} \in \mathbb{S}^1$ is also an infinite equilibrium point. On the other hand the local behavior near $-\mathbf{s}$ is the local behavior near $\mathbf{s}$ multiplied by $(-1)^{d-1}$.

2.2. **Equilibrium points.** Let q be an equilibrium point of $p(\mathcal{X})$. If the linear part of $p(\mathcal{X})$ at q is identically zero, and it is an isolated equilibrium point, we call q a *linearly zero equilibrium point*. We will use the special changes of variables called *blow-up's* for studying the local phase portrait of this kind of equilibrium points. For more details about the blow-up's see [1].

In addition we can compute the topological indices of the finite and infinite equilibrium points which sometimes help for determining their local phase portraits. Here we will present two important theorems, the Poincaré Formula and the Poincaré–Hopf Theorem, see for more details Chapter 6 of [14].

Theorem 2.1 (Poincaré Formula)**.** *Let q be an isolated equilibrium point having the finite sectorial decomposition property. Let e, h and p denote the number of elliptic, hyperbolic and parabolic sectors of q, respectively. Then the index of q is $(e - h)/2 + 1$.*

Corollary 2.2. *The index of a node, a center, a saddle and a cusp are* 1, 1, -1 *and* 0*, respectively.*

Theorem 2.3 (Poincaré–Hopf Theorem)**.** *For every vector field on the sphere* $\mathbb{S}^2$ *with a finite number of equilibrium points, the sum of the indices of all its equilibria is* 2*.*

We have the following remark.

Remark 2.4. *Since the flow of Hamiltonian systems preserves the area, we have that any finite equilibrium of Hamiltonian systems must be either a center, or union of an even number of hyperbolic sectors. In particular, the finite nilpotent equilibrium points of Hamiltonian planar polynomial vector fields are either saddles, centers, or cusps, for more details see Theorem 3.5 of* [14].

The *separatrix skeleton* of a vector field $p(\mathcal{X})$ in the Poincaré disk is the union of all its separatries together with an orbit from each one of its canonical regions. We say that two separatrix skeletons are topologically *equivalent* if there exists a homeomorphism from one to the other which sends orbits to orbits preserving or reversing the direction of all orbits. From Markus [20], Neumann [22] and Peixoto [23], we present the following theorem which shows that is enough to describe the separatrix skeleton in order to determine the topological equivalence class of a vector field $p(\mathcal{X})$ in the Poincaré disk.

Theorem 2.5 (Markus–Neumann–Peixoto Theorem)**.** *Assume that* $(\mathbb{D}^2, \phi_1)$ *and* $(\mathbb{D}^2, \phi_2)$ *are two continuous flows with only isolated singular points. Then these flows are topologically equivalent if and only if their separatrix skeletons are equivalent.*

3. Proof of Theorem 1.1

If $P(x) = a$ and $Q(x, y) = Ax^2 + By^2 + C$ with $aAB \neq 0$, we have $V(x, y) = \frac{1}{Ax^2/a+By^2/a+C/a}$. Without loss of generality we can take $a = 1$, and then the rational Hamiltonian function given in statement of Theorem 1.1 is

$$H_1(x, y) = \frac{y^2}{2} + \frac{1}{Ax^2 + By^2 + C}.$$

The associated Hamiltonian system for this new Hamiltonian function $H_1(x, y)$ is

$$\dot{x} = y - \frac{2By}{(Ax^2 + By^2 + C)^2}, \qquad \dot{y} = \frac{2Ax}{(Ax^2 + By^2 + C)^2}. \tag{11}$$

We see that system (11) is invariant under the symmetries $(x, y, t) \to (x, -y, -t)$ and $(x, y, t) \to (-x, y, -t)$, i.e., the orbits of the phase portraits are symmetric with respect to the x-axis and the y-axis.

We apply the time rescaling $dt = (Ax^2 + By^2 + C)^2 d\tau$, and system (11) becomes

$$x' = y(Ax^2 + By^2 + C)^2 - 2By, \qquad y' = 2Ax. \tag{12}$$

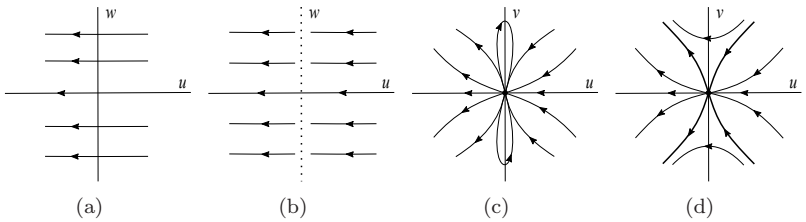

FIGURE 3. Blow-up of the origin of system (13) when $AB > 0$. (a) System (15), (b) System (14), (c) System (13) with $A > 0$, (d) System (13) with $A < 0$.

Through the Poincaré compactification we study the local phase portraits of the infinite equilibrium points of system (12). In the local chart U_1 system (12) becomes

$$\begin{aligned} u' =& -u^2(A+Bu^2)^2 - 2Cu^2(A+Bu^2)v^2 + (2B-C^2)u^2v^4 + 2Av^4, \\ v' =& -vu((A+Bu^2)^2 + 2Bcu^2v^2 + 2ACv^2 + (C^2-2B)v^4). \end{aligned} \tag{13}$$

(i) At infinity, i.e. on $v = 0$, there is only one equilibrium point in U_1 when $AB > 0$, namely $O' = (0, 0)$. The linear part of system (13) on $v = 0$ is

$$\begin{pmatrix} -2u(A+Bu^2)(A+3Bu^2) & 0 \\ 0 & -u(A+Bu^2)^2 \end{pmatrix}.$$

Thus the linear part of the equilibrium O' is identically zero. For studying the local phase portrait at the equilibrium O' we do the blow-up $(u, v) \to (u, w)$ with $w = v/u$. Then we have the system

$$\begin{aligned} u' =& -u^2((A+Bu^2)^2 + 2Cu^2(A+Bu^2)w^2 - 2Au^2w^4 + (C^2-2B)u^4w^4), \\ w' =& -2Au^3w^5. \end{aligned} \tag{14}$$

By a rescaling of the time we eliminate the common factor u^2 between u' and w' and obtain the system

$$\begin{aligned} u' =& -((A+Bu^2)^2 + 2Cu^2(A+Bu^2)w^2 - 2Au^2w^4 + (C^2-2B)u^4w^4), \\ w' =& -2Auw^5. \end{aligned} \tag{15}$$

System (15) does not have equilibria on $u = 0$. Thus we study the local phase portrait in the neighborhood $u = 0$. Note that $u'|_{u=0} = -A^2$ and $w'|_{u=0} = 0$ showing that the flow is decreasing in the u direction, see Figure 3(a). Going back through the change of variables until system (13), as in the pass from system (15) to system (14) does not change the local phase portrait of system (14) except that the w-axis becomes filled with equilibrium points, see Figure 3(b). Taking into account the flow of system (13) on the axes we have $u'|_{v=0} = -A^2u^2 + O(u^3)$, $u'|_{u=0} = 2Av^4$ and $v'|_{u=0} = 0$. Then we see that the equilibrium point O' consists of two elliptic sectors and two parabolic sectors when $A > 0$, as it is shown in Figure 3(c). And it has two hyperbolic sectors and two parabolic sectors when $A < 0$, see Figure 3(d).

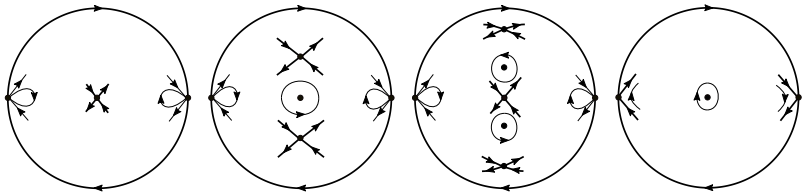

FIGURE 4. Local phase portraits at the equilibrium points of system (12) with $AB > 0$. (a) If $A > 0$, $B > 0$ and $C \geq \sqrt{2B}$, (b) If $A > 0$, $B > 0$ and $-\sqrt{2B} \leq C < \sqrt{2B}$, (c) If $A > 0$, $B > 0$ and $C < -\sqrt{2B}$ (d) If $A < 0$ and $B < 0$.

Now we check if the origin of the local chart U_2 is an equilibrium point. In U_2 we use (9) to get

$$\begin{aligned} u' =& (B + Au^2)^2 + 2C(B + Au^2)v^2 - 2Au^2v^4 + (C^2 - 2B)v^4, \\ v' =& -2Auv^5. \end{aligned} \tag{16}$$

Clearly the origin of U_2 is not an equilibrium point.

Thus system (12) has two equilibrium points at infinity, the point O' in U_1 and its diametrically opposite O'' in V_1, which have the same sense. The index of O' (O'') is 2 and 0 when $A > 0$ and $A < 0$, respectively. On the other hand, the set $L = \{(x, y)|Ax^2 + By^2 + C = 0\}$ is empty when $AC > 0$. And this set is a point $(0, 0)$ or an ellipse when $C = 0$ or $AC < 0$, respectively.

Now we study the finite equilibria of systems (11) and (12) in two subcases: (i.a) $A > 0$ and $B > 0$, (i.b) $A < 0$ and $B < 0$.

(i.a.1) If $C \geq \sqrt{2B}$ system (12) has one equilibrium point $p_1 = (0, 0)$. We can get that p_1 is a saddle because its eigenvalues are $\lambda_{1,2} = \pm\sqrt{2A(C^2 - 2B)}$. In particular the equilibrium point p_1 is nilpotent when $C = \sqrt{2B}$. From Theorem 2.3 and Remark 2.4 we obtain that the nilpotent point p_1 must be a saddle. Since the sum of the indices of all the infinite and finite equilibria is 2, we have that the local phase portraits at the equilibria of system (12) are shown in Figure 4(a). Therefore in this case the global phase portrait of the smooth Hamiltonian system (11) is topologically equivalent to the one of 1.1 of Figure 1.

(i.a.2) If $-\sqrt{2B} \leq C < \sqrt{2B}$ system (12) has three finite equilibrium points $p_1 = (0, 0)$ and $p_{2,3} = (0, \pm\sqrt{(\sqrt{2B} - C)/B})$. The equilibrium point p_1 is a center because its eigenvalues $\lambda_{1,2}$ are a pair of pure imaginary numbers when $C \neq -\sqrt{2B}$. In particular p_1 is nilpotent when $C = -\sqrt{2B}$, and we obtain that this point must be a center so that the sum of indices of all equilibria is 2, see Theorem 2.3 and Remark 2.4. And the equilibria $p_{2,3}$ are two saddles because their eigenvalues are $\lambda_{3,4} = \pm 2\sqrt{A(4B - 2C\sqrt{2B})}$. Then we have the local phase portraits at these equilibrium points of system (12) in Figure 4(b). Since the energy levels at the saddles $p_{2,3}$ are equal and using the symmetries of system (12), the two saddles $p_{2,3}$

must be on the boundary of the period annulus of the center at p_1. If $0 < C < \sqrt{2B}$ the set L is empty, and the Hamiltonian system (11) is smooth. Then we have the phase portrait 1.2 of Figure 1. Otherwise, the Hamiltonian system (11) is discontinuous. If $C = 0$ the equilibrium point p_1 is virtual point because it is in the set $L = \{(0, 0)\}$. Hence we have the phase portrait 1.3 of Figure 1. If $-\sqrt{2B} < C < 0$ the set L in the Poincaré disk is an ellipse. Substituting the coordinates of $p_{2,3}$ into the set L we have $Ax^2 + By^2 + C = \sqrt{2B} \neq 0$, which means the equilibria $p_{2,3}$ are not in the set L. Therefore in this subcase the phase portrait is topologically equivalent to the one of 1.4 of Figure 1.

(i.a.3) If $C < -\sqrt{2B}$ system (12) has five finite equilibrium points $p_1 = (0, 0)$, $p_{2,3} = (0, \pm\sqrt{(\sqrt{2B} - C)/B})$ and $p_{4,5} = (0, \pm\sqrt{(-\sqrt{2B} - C)/B})$. The equilibria $p_{1,2,3}$ are saddles because their eigenvalues are a pair of opposite numbers, and $p_{4,5}$ are centers because their eigenvalues are $\lambda_{5,6} = \pm 2\sqrt{A(4B + 2C\sqrt{2B})}$. We have that the local phase portraits at the equilibria of system (12) are shown in Figure 4(c). Since the energy levels at the saddles $p_{2,3}$ are equal and by the symmetries of system (12), one unstable and one stable separatrices of the saddle p_2 must cross the x-axis and connect with the stable and unstable separatrices of the saddle p_3. On the other hand, the set L in the Poincaré disk is an ellipse, and the equilibrium points p_i $(i = 1, 2, 3, 4, 5)$ are not in this set. Thus the saddle p_1 must be on the boundary of the period annulus of the two centers $p_{4,5}$. Therefore system (11) is a discontinuous Hamiltonian system and we have the phase portrait 1.5 of Figure 1.

(i.b) Assume that $A < 0$ and $B < 0$, system (12) has only one equilibrium point $p_1 = (0, 0)$, and it is a center. We obtain the local phase portraits of system (12) at its equilibria in the Poincaré disk, see Figure 4(d). If $C > 0$ the set L in the Poincaré disk is an ellipse, the phase portrait of the discontinuous Hamiltonian system (11) is topologically equivalent to the one shown in 1.6 of Figure 1. If $C = 0$ the set L in the Poincaré disk is one point $(0, 0)$, hence p_1 is a virtual point. Then the phase portrait of system (11) is topologically equivalent to the one shown in 1.7 of Figure 1. If $C < 0$ the set L is empty, then system (11) is a smooth Hamiltonian system and we obtain the phase portrait 1.8 of Figure 1.

(ii) Next we consider the case $AB < 0$, system (13) has three equilibrium points $O' = (0, 0)$, $M' = (\sqrt{-A/B}, 0)$ and $N' = (-\sqrt{-A/B}, 0)$ in U_1, which are linearly zero. Similarly to the above case, the local phase portrait of O' is shown in Figure 3(c) and 3(d) when $A > 0$ and $A < 0$, respectively. Now we move the equilibrium point M' to the origin doing the change of variables $(u, v) \to (u + \sqrt{-A/B}, v)$. Then we have the system

$$
\begin{aligned}
u' =& -B^2u^2(\sqrt{-A/B} + u)^2(2\sqrt{-A/B} + u)^2 + 2Av^4 \\
& - 2BCuv^2(\sqrt{-A/B} + u)^2(2\sqrt{-A/B} + u) \\
& + (2B - C^2)v^4(\sqrt{-A/B} + u)^2, \\
v' =& -v(\sqrt{-A/B} + u)(B^2u^2(2\sqrt{-A/B} + u)^2 + 2ACv^2 \\
& + (C^2 - 2B)v^4 + 2BCv^2(\sqrt{-A/B} + u)^2).
\end{aligned} \tag{17}
$$

Applying the blow-up technique and taking into account the flow of system (17) on the axes, we obtain that the local phase portrait at the origin of system (17) has

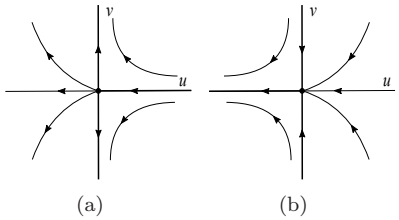

FIGURE 5. Local phase portrait at the origin of systems (17) and (18). (a) System (17) with $2B - C^2 \geq 0$, or System (18) with $2B - C^2 < 0$, (b) System (17) with $2B - C^2 < 0$, or System (18) with $2B - C^2 \geq 0$.

two hyperbolic sectors and one parabolic sector, as it is shown in Figure 5(a) and 5(b) when $2B - C^2 \geq 0$ and $2B - C^2 < 0$, respectively.

Similarly doing the change of variables $(u, v) \to (u - \sqrt{-A/B}, v)$ we move the equilibrium point N' to the origin and have

$$
\begin{aligned}
u' =& -B^2u^2(\sqrt{-A/B}-u)^2(2\sqrt{-A/B}-u)^2 + 2Av^4 \\
&+ 2BCuv^2(\sqrt{-A/B}-u)^2(2\sqrt{-A/B}-u) \\
&+ (2B-C^2)v^4(\sqrt{-A/B}-u)^2, \\
v' =& v(\sqrt{-A/B}-u)(B^2u^2(2\sqrt{-A/B}-u)^2 + 2ACv^2 \\
&+ (C^2-2B)v^4 + 2BCv^2(\sqrt{-A/B}-u)^2).
\end{aligned} \tag{18}
$$

The local phase portrait at the origin of system (18) consists of two hyperbolic sectors and one parabolic sector, see Figure 5(a) and 5(b) when $2B - C^2 < 0$ and $2B - C^2 \geq 0$ respectively.

From system (16) we have that the origin of U_2 is not an equilibrium point. Thus system (12) has six infinite equilibrium points. Three equilibrium points O', M' and N' in U_1, and their diametrically opposite O'', M'' and N'' in V_1. The phase portraits in the charts $V_{1,2}$ have the same sense than in $U_{1,2}$ respectively, because the degree of system (12) is 5. When $C = 0$ we obtain that the set $L = \{(x, y)|Ax^2+By^2+C = 0\}$ corresponds to a couple of straight lines $y = \pm\sqrt{-A/B}x$ in the Poincaré disk, which intersect at point $(0, 0)$. Because the set L becomes $\{(u, v)|A + Bu^2 = 0\}$ by the Poincaré transformations $(x, y) \to (1/v, u/v)$, i.e. one straight line connects M' and M'', and one connects N' and N''. If $AC > 0$ the set L corresponds to a hyperbola in the Poincaré disk, which connects M' and N'', or N' and M'', respectively. Similarly if $AC < 0$ the set L corresponds to a hyperbola connecting M' and N', or M'' and N'', respectively. Therefore in these three cases there are only two infinite equilibrium points O' and O'' for the discontinuous Hamiltonian system (11).

Now we focus on the finite equilibrium points of system (12) and of the discontinuous Hamiltonian system (11). From the previous analysis system (12) can has

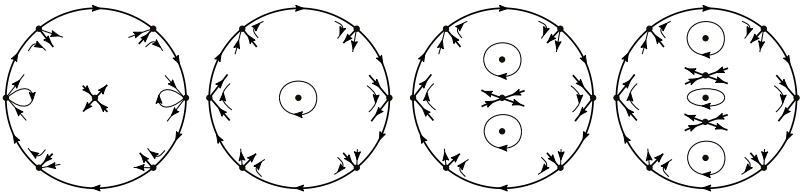

FIGURE 6. Local phase portraits at the equilibrium points of system (12) with $AB < 0$. (a) If $A > 0$ and $B < 0$, (b) If $A < 0$, $B > 0$ and $\sqrt{2B} \leq C$, (c) If $A < 0$, $B > 0$ and $-\sqrt{2B} \leq C < \sqrt{2B}$, (d) If $A < 0$, $B > 0$ and $C < -\sqrt{2B}$.

five finite equilibrium points, namely

$$p_1 = (0,0), \qquad p_{2,3} = (0, \pm\sqrt{(\sqrt{2B} - C)/B}), \qquad p_{4,5} = (0, \pm\sqrt{(-\sqrt{2B} - C)/B}).$$

(ii.a) Assume that $A > 0$ and $B < 0$, system (12) has one equilibrium point p_1, and it is a saddle because its eigenvalues are $\lambda_{1,2} = \pm\sqrt{2A(C^2 - 2B)}$. The local phase portrait at the infinite and finite equilibrium points of system (12) in Poincaré disk is shown in Figure 6(a). From the previous analysis we obtain that the phase portraits of the discontinuous Hamiltonian system (11) are topologically equivalent to the ones shown in 1.9, 1.10 and 1.11 of Figure 1 when $C > 0$, $C = 0$ and $C < 0$, respectively. In particular the point p_1 is a virtual saddle when $C = 0$.

(ii.b) Assume that $A < 0$ and $B > 0$.

(ii.b.1) If $\sqrt{2B} \leq C$ system (12) has only one equilibrium point p_1, which is a center, in particular it is a nilpotent center when $C = \sqrt{2B}$. The local phase portraits at the equilibria of system (12) are shown in Figure 6(b). Going back to the rational Hamiltonian system (11), the infinite equilibria M', M'', N' and N'' are virtual points, because the set L in the Poincaré disk is a hyperbola connecting either the points M' and N', or M'' and N''. Hence in this subcase the phase portrait of the discontinuous Hamiltonian system (11) is topologically equivalent to the one shown in 1.12 of Figure 1.

(ii.b.2) If $-\sqrt{2B} \leq C < \sqrt{2B}$ system (12) has three equilibrium points $p_{1,2,3}$. From the linear part of system (12) we obtain that p_1 is a saddle, and $p_{2,3}$ are two centers with eigenvalues $\lambda_{3,4} = \pm 2\sqrt{A(4B - 2C\sqrt{2B}}$. In particular the equilibrium point p_1 is a nilpotent saddle when $C = -\sqrt{2B}$. And it has six infinite equilibria O', O'', M', M'', N' and N'', the local phase portraits of these equilibria are given in Figure 6(c). Going back to the rational Hamiltonian system (11), in the case $0 < C < \sqrt{2B}$ the set L in the Poincaré disk formed by a hyperbola connecting either the points M' and N', or M'' and N''. In addition the equilibrium points $p_{1,2,3}$ are not in L. Therefore the saddle p_1 must be on the boundary of the period annulus of the two centers $p_{2,3}$. In this subcase the phase portrait of the

discontinuous Hamiltonian system (11) is topologically equivalent to the one shown in 1.13 of Figure 1.

When $C = 0$ the set L in the Poincaré disk is two straight lines intersecting at the point $(0, 0)$, which connect either the points M' and M'', or N'' and N''. Hence the finite point p_1 and the infinite points M', M'', N' and N'' are virtual points. Therefore the phase portrait in this case turns out to be topologically equivalent to 1.14 of Figure 1. In the subcase $-\sqrt{2B} \leq C < 0$ the set L in the Poincaré disk is a hyperbola connecting either the points M' and N'', or N' and M''. We obtain that the phase portrait is topologically equivalent to the one of 1.15 of Figure 1.

(ii.b.3) If $C < -\sqrt{2B}$ system (12) has five equilibrium points p_i $(i = 1, 2, 3, 4, 5)$. We obtain that $p_{1,2,3}$ are centers and $p_{4,5}$ are saddles from the linear part of system (12). The local phase portraits of system (12) at its finite and infinite equilibrium points are topologically equivalent to the one of Figure 6(d). Going back to the rational Hamiltonian system (11), infinite equilibria M', M'', N' and N'' are virtual points, because they are in set L. On the other hand, all finite equilibria are not in the set L.

If one stable and one unstable separatrices of p_4 cross the x-axis and connect with the unstable and the stable separatrices of p_5, respectively, then they form a heteroclinic loop surrounding the center at origin. With the previous information the phase portrait of the Hamiltonian system (11) is topologically equivalent to the one shown in 1.16 of Figure 1.

If one stable and one unstable separatrices of p_4 connect with the unstable separatrix of O'' and the unstable separatrix of O' respectively. By the symmetries the analogous happens with the separatrix of p_5. The phase portrait of system (11) in this subcase is topologically equivalent to 1.17 of Figure 1.

If one stable and one unstable separatrices of p_4 connect with O'' and O' respectively. And the stable and the unstable separatrices of O'' connect with the unstable and the stable separatrices of O', respectively. By the symmetries we obtain the phase portrait 1.18 of Figure 1.

This completes the proof of Theorem 1.1.

4. Proof of Theorem 1.2

Next we study the SD Hamiltonian system $H_2(x, y)$ with $aAB \neq 0$, without loss of generality we can take $a = 1$, the new Hamiltonian system of $H_2(x, y)$ becomes

$$\dot{x} = y - \frac{2Bxy}{(Ax^2 + By^2 + C)^2}, \qquad \dot{y} = \frac{Ax^2 - By^2 - C}{(Ax^2 + By^2 + C)^2}. \tag{19}$$

System (19) is invariant under the transformation

$$(x, y, A, B, C, t) \to (-x, y, -A, -B, -C, -t),$$

hence we only need to study the phase portraits of system (19) with $B > 0$. On the other hand we note that system (19) is invariant under the symmetry $(x, y, t) \to (x, -y, t)$, i.e., the orbits of the phase portraits are symmetric with respect to the x-axis.

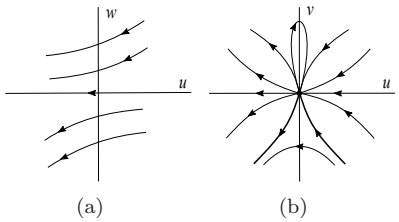

FIGURE 7. Blow-up of the origin of system (21) when $A > 0$. (a) System (22), (b) System (21).

Applying the rescaling $dt = (Ax^2 + By^2 + C)^2 d\tau$, system (19) becomes

$$x' = -2Bxy + y(Ax^2 + By^2 + C)^2, \qquad y' = Ax^2 - By^2 - C, \tag{20}$$

which is a polynomial differential system of degree 5. System (20) in the local chart U_1 is

$$\begin{aligned} u' =& -u^2(A + Bu^2)^2 - 2Cu^2v^2(A + Bu^2) + Av^3 + u^2v^3(B - C^2v) - Cv^5, \\ v' =& -uv((A + Bu^2)^2 + 2Cv^2(A + Bu^2) - v^3(2B - C^2v)). \end{aligned} \tag{21}$$

For $v = 0$ there are three possible equilibrium points in U_1: $O' = (0, 0)$, $M' = (\sqrt{-A/B}, 0)$ and $N' = (-\sqrt{-A/B}, 0)$.

(i) When $A > 0$ the origin of system (21) is the unique infinite equilibrium point in U_1 and it is linearly zero. In order to determine its local phase portrait, we do the directional blow-up $(u, v) \to (u, w)$ with $w = v/u$. And after eliminating the common factor u^2 between u' and w' we have

$$\begin{aligned} u' =& -(A + Bu^2)^2 - 2Cu^2(A + Bu^2)w^2 + Auw^3 \\ & + (B - C^2uw - Cw^2)u^3w^3, \\ w' =& w^4(-A + Bu^2 + Cu^2w^2). \end{aligned} \tag{22}$$

For $u = 0$ this system does not have any equilibrium points, therefore we analyze the vector field in a neighborhood of $u = 0$. Note that $u'|_{w=0} = -A^2 < 0$. Then the local phase portrait at the origin of system (22) is given in Figure 7(a). We reconstruct the flow through the blow-up and taking into account the behavior of system (21) on the axes near the origin, it has one elliptic sector, one hyperbolic sector and two parabolic sectors, see Figure 7(b).

In the local chart U_2 system (20) has the form

$$\begin{aligned} u' =& (B + Au^2)^2 + 2C(B + Au^2)v^2 - u(B + Au^2)v^3 + Cv^4(C + uv), \\ v' =& v^4(B - Au^2 + Cv^2). \end{aligned} \tag{23}$$

The origin is not an equilibrium point of system (23).

In summary, for $A > 0$ system (20) has two infinite equilibrium points, the point O' in U_1 and its diametrically opposite O'' in V_1, which have the same sense. The set $L = \{(x, y) | Ax^2 + By^2 + C = 0\}$ is empty when $C > 0$. And it is a point $(0, 0)$ or an ellipse when $C = 0$ or $C < 0$, respectively.

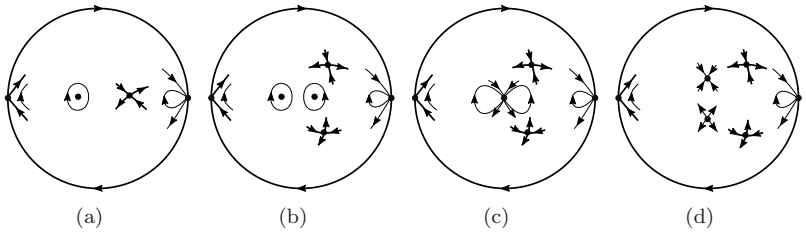

FIGURE 8. The local phase portraits at the equilibrium points of system (20) with $A > 0$. (a) If $C \geq \sqrt[3]{B^2/(4A)}$, (b) If $0 < C < \sqrt[3]{B^2/(4A)}$, (c) If $C = 0$, (d) If $C < 0$.

Now we study the finite equilibria of systems (19) and (20). From the following analysis we know that in the Poincaré disk the local phase portraits at all equilibrium points depend on C, as it is shown in Figure 8.

(i.a) If $C \geq \sqrt[3]{B^2/(4A)}$ system (20) has two equilibria $p_{1,2} = (\pm\sqrt{C/A}, 0)$. Since the eigenvalues of the equilibrium points $p_{1,2}$ are $\lambda_{1,2} = \pm 2\sqrt{C(2\sqrt{AC^3} - B)}$ and $\lambda_{3,4} = \pm 2\sqrt{-C(2\sqrt{AC^3} + B)}$, they are a saddle and a center, respectively. We have that the local phase portraits at these equilibria in Poincaré disk are shown in Figure 8(a). In particular the equilibrium p_1 is nilpotent when $C = \sqrt[3]{B^2/(4A)}$, by Theorem 2.3 and Remark 2.4, p_1 is also a saddle so that the sum of the indices of all equilibria is 2 in the Poincaré sphere. Hence in this subcase we have the phase portrait 1.19 of Figure 1.

(i.b) If $0 < C < \sqrt[3]{B^2/(4A)}$ we can get four equilibria $p_{1,2} = (\pm\sqrt{C/A}, 0)$ and

$$p_{3,4} = (\sqrt[3]{B/(2A^2)}, \pm\sqrt{(\sqrt[3]{2B^2} - 2\sqrt[3]{A}C)/(2B\sqrt[3]{A})}).$$

The equilibria $p_{1,2}$ are two centers because their eigenvalues are a pair of pure imaginary numbers. And the equilibrium points $p_{3,4}$ are two saddles because their eigenvalues are $\lambda_{5,6} = \pm\sqrt{6}\sqrt[3]{B}\sqrt{\sqrt[3]{2B}(\sqrt[3]{B^2/A} - \sqrt[3]{4}C)}$. We obtain the local phase portraits of all equilibria in the Poincaré disk, see Figure 8(b). The energy level $H_2(x, y) = h$ at the saddles $p_{3,4}$ are equal. One stable and one unstable separatrices of the saddle p_3 must cross the x-axis because it cannot intersect the unstable separatrix of itself, then they connect with one unstable and one stable separatrices of the saddle p_4, respectively. And it provides a heteroclinic loop surrounding the center p_1. Hence in this subcase we have the phase portrait 1.20 of Figure 1.

(i.c) If $C = 0$ system (20) has three equilibrium points $p_1' = (0, 0)$ and $p_{3,4}' = (\sqrt[3]{B/(2A^2)}, \pm\sqrt[6]{1/(4AB)})$, where p_1' is linearly zero and $p_{3,4}'$ are two saddles. We apply the directional blow-up $(x, y) \to (x, w)$ with $w = y/x$. And after eliminating the common factor x between x' and w' we have

$$x' = xw(-2B + (A + Bw^2)^2x^3), \qquad w' = -(A + Bw^2)(-1 + w^2(A + Bw^2)x^3). \tag{24}$$

System (24) does not have equilibrium points for $x = 0$. We study the local phase portrait in the neighborhood $w = 0$. Note that $x'|_{w=0} = 0$ and $w'|_{w=0} = A$ showing that the flow is increase in the w direction, see Figure 9(a). Going back through

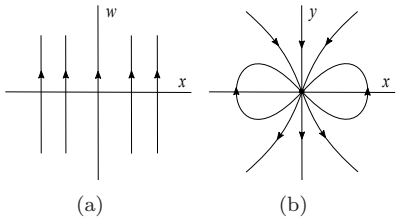

FIGURE 9. Blow-up of the origin of system (20) when $A > 0$ and $C = 0$. (a) System (24), (b) system (20).

the blow-up and taking into account the behavior of the flow on the axes, i.e. $x'|_{y=0} = 0$, $y'|_{y=0} = Ax^2 > 0$ and $y'|_{x=0} = -By^2 < 0$, we obtain the local phase portrait at the origin of system (20). It has two elliptic sectors and two parabolic sectors, as it is shown in Figure 9(b).

We obtain the local phase portraits at all equilibria in the Poincaré disk, as it is shown in Figure 8(c). Similarly to the case (i.b) one stable separatrix of the saddle p_3' must connect with one unstable separatrix of the saddle p_4'. In addition one unstable separatrix of the saddle p_3' connects with the origin. By symmetry the analogous happens with the separtrices of p_4'. Going back to the rational Hamiltonian system (19), p_1' is a virtual point. Thus we obtain the phase portrait of system (19) is topologically equivalent to 1.21 of Figure 1.

(i.d) If $C < 0$ system (20) has four equilibria $p_{3,4}$ and $p_{5,6} = (0, \pm\sqrt{-C/B})$. From case (i.b) we have that the equilibria $p_{3,4}$ are two saddles. And the equilibria $p_{5,6}$ are an attracting node and a repelling node, because their eigenvalues are $\lambda_{7,8} = -2\sqrt{-BC}$ and $\lambda_{9,10} = 2\sqrt{-BC}$, respectively. Similarly to the above case, we get the local phase portraits at all equilibria of system (20), see Figure 8(d). Going back to the Hamiltonian system (19), $p_{5,6}$ are two virtual equilibrium points because they are in the L. Hence in this case the phase portrait is topologically equivalent to 1.22 of Figure 1.

(ii) We obtain that in the case $A < 0$ system (21) has three equilibria O', M' and N' in U_1, which are linearly zero. Similarly to case (i) we obtain that the local phase portrait at O' has one elliptic sector, one hyperbolic sector and two parabolic sectors, as it is shown in Figure 10(a).

In order to study the infinite point M', we translate it to the origin doing the change of variables $(u, v) \to (u + \sqrt{-A/B}, v)$, system (21) becomes

$$\begin{aligned} u' =& -B^2u^2(\sqrt{-A/B}+u)^2(2\sqrt{-A/B}+u)^2 + Av^3 \\ & - 2BCv^2u(\sqrt{-A/B}+u)^2(2\sqrt{-A/B}+u) - Cv^5 \\ & + v^3(B - C^2v)(\sqrt{-A/B}+u)^2, \\ v' =& -(u+\sqrt{-A/B})v(B^2u^2(2\sqrt{-A/B}+u)^2 - v^3(2B - C^2v) \\ & + 2BCv^2u(2\sqrt{-A/B}+u)). \end{aligned} \tag{25}$$

Applying the directional blow-up technique and taking into account the behavior of the flow on the axes, i.e. $u'|_{v=0} = -4A^2u^2 + O(u^3)$ and $v'|_{u=0} = 2B\sqrt{-A/B}v^4 +$

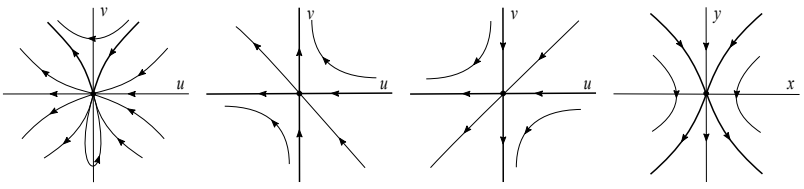

FIGURE 10. Local phase portrait at the origin of systems (21), (25), (26) and (20) when $A < 0$. (a) System (21), (b) System (25), (c) System (26), (d) System (20) with $C = 0$.

$O(v^5)$, we obtain that the local phase portrait at the origin of system (25) has two hyperbolic sectors and two parabolic sectors, it is given in Figure 10(b).

Similarly we translate the point N' to the origin doing the change of variables $(u, v) \to (u - \sqrt{-A/B}, v)$, the system writes

$$\begin{aligned} u' =& -B^2u^2(\sqrt{-A/B}-u)^2(2\sqrt{-A/B}-u)^2 + Av^3 \\ &+ 2BCv^2u(\sqrt{-A/B}-u)^2(2\sqrt{-A/B}-u) - Cv^5 \\ &+ v^3(B-C^2v)(\sqrt{-A/B}-u)^2, \\ v' =& -(u-\sqrt{-A/B})v(B^2u^2(2\sqrt{-A/B}-u)^2 + v^3(-2B+C^2v) \\ &- 2BCv^2u(2\sqrt{-A/B}-u)). \end{aligned} \tag{26}$$

The local phase portrait at the origin of system (26) has two hyperbolic sectors and two parabolic sectors, see Figure 10(c).

From system (23) the origin is not an equilibrium point in the chart U_2. Thus the associated polynomial system (20) has six infinite equilibrium points, three equilibrium points O', M' and N' in U_1, and their diametrically opposite points O'', M'' and N'' in V_1, which have the same sense respectively. When $C = 0$ we obtain that the set $L = \{(x, y)|Ax^2 + By^2 + C = 0\}$ corresponds to a couple of straight lines $y = \pm\sqrt{-A/B}x$ connecting M' with M'', and N' with N''. If $C < 0$ the set L is a hyperbola, which connects M' and N'', or N' and M''. If $C > 0$ the set L is also a hyperbola connecting M' and N', or M'' and N''. Therefore in these three cases there are only two infinite equilibrium points O' and O'' for the discontinuous Hamiltonian system (19).

Now we study the finite equilibria of systems (19) and (20). From the following analysis we obtain that system (20) has at most six finite equilibrium points, as

$$\begin{aligned} p_{1,2} =& (\pm\sqrt{C/A}, 0), \qquad p_{5,6} = (0, \pm\sqrt{-C/B}), \\ p_{3,4} =& (\sqrt[3]{B/(2A^2)}, \pm\sqrt{(\sqrt[3]{2B^2} - 2\sqrt[3]{A}C)/(2B\sqrt[3]{A})}). \end{aligned}$$

(ii.a) If $C > 0$ system (20) has no finite equilibrium points. From the previous analysis the point M', M'', N' and N'' are virtual points, where M' and N', M'' and N'' are connected by a hyperbola. Hence the phase portrait of system (19) in this subcase is topologically equivalent to 1.23 of Figure 1.

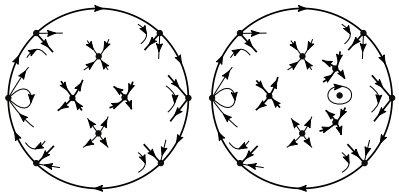

FIGURE 11. The local phase portraits at the equilibrium points of system (20) with $A < 0$. (a) If $\sqrt[3]{B^2/(4A)} \leq C < 0$, (b) If $C < \sqrt[3]{B^2/(4A)}$.

(ii.b) If $C = 0$ system (20) has one equilibrium point $p_1' = (0, 0)$, which is linearly zero. Similarly to the case (i.c) doing the blow-up technique we obtain that the origin consists of two hyperbolic sectors, one attracting parabolic sector and one repelling parabolic sector, as it is shown in Figure 10(d). Going back to system (19) the point p_1' is a virtual point, because it is in the set L. Hence we have the phase portrait 1.24 of Figure 1.

(ii.c) If $\sqrt[3]{B^2/(4A)} \leq C < 0$ system (20) has four equilibria $p_{1,2,5,6}$, which are two saddles, an attracting hyperbolic node and a repelling hyperbolic node, their eigenvalues can see case (i.a) and (i.d). In particular, p_1 is a nilpotent saddle when $C = \sqrt[3]{B^2/(4A)}$ so that the sum of the indices of all equilibria is 2 in Poincaré sphere. Thus we have the local phase portraits of system (20) at all equilibria in the Poincaré disk, see Figure 11(a). Using the previous analysis we obtain that the stable separatrices of the saddle p_1 connect with the node p_6 and the infinite equilibrium point M', and the unstable ones must connect with the node p_5 and the infinite equilibrium point N'. Similarly the unstable and stable separatrices of the saddle p_2 must connect with p_5 and p_6, respectively. And the other two separatrices of p_2 connect with the infinite equilibrium point O''. Going back to the discontinuous Hamiltonian system (19) the points $p_{5,6}$ are two virtual points. Therefore in this subcase we have the phase portrait 1.25 of Figure 2.

(ii.d) If $C < \sqrt[3]{B^2/(4A)}$ system (20) has six equilibria p_i $(i = 1, 2, \cdots, 6)$, where p_1 is a center, $p_{2,3,4}$ are hyperbolic saddles, p_5 is an attracting hyperbolic node and p_6 is a repelling hyperbolic node. The local phase portraits of system (20) at its equilibria in the Poincaré disk are topologically equivalent to the one of Figure 11(b). We have that the saddles $p_{3,4}$ must be on the boundary of the period annulus of the center p_1, because it cannot intersect the stable separatrix of itself and the energy level $H_2(x, y) = h$ at the saddles $p_{3,4}$ are equal. Hence it provides a heteroclinic loop surrounding the center p_1. In addition one unstable separatrix of p_3 and one stable separatrix of p_4 connect with the equilibria p_5 and p_6, respectively. And one unstable and one stable separatrices of the saddle p_2 must connect with p_5 and p_6, respectively. We have that the equilibria $p_{5,6}$, M', M'', N' and N'' are virtual points of the discontinuous Hamiltonian system (19). Hence in this subcase the phase portrait is topologically equivalent to 1.26 of Figure 2.

This concludes the proof of Theorem 1.2.

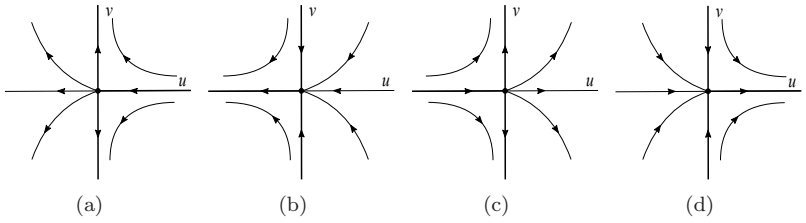

FIGURE 12. Local phase portrait at the origin of systems (30) and (31). (a) System (30) with $B > 0$, (b) System (30) with $B < 0$, (c) System (31) with $B > 0$, (d) System (31) with $B < 0$.

5. Proof of Theorem 1.3

For $V(x, y) = \frac{ax^2}{Ax^2+By^2+C}$ with $aAB \neq 0$, we can take without loss of generality $a = 1$, and have the associate system of $H_3(x, y)$

$$\dot{x} = y - \frac{2Bx^2y}{(Ax^2 + By^2 + C)^2}, \qquad \dot{y} = \frac{-2x(C + By^2)}{(Ax^2 + By^2 + C)^2}. \tag{27}$$

The orbits of the phase portraits of the SD Hamiltonian system (27) are symmetric with respect to the axes, because system (27) is invariant under the symmetries $(x, y, t) \to (x, -y, t)$ and $(x, y, t) \to (-x, y, t)$. Now we consider the following two cases: (i) $C = 0$ and (ii) $C \neq 0$.

(i) Assume that $C = 0$, by the rescaling $dt = (Ax^2 + By^2)^2 d\tau/y$, system (27) becomes

$$x' = (Ax^2 + By^2)^2 - 2Bx^2, \qquad y' = -2Bxy. \tag{28}$$

System (28) in U_1 has the form

$$u' = -u(A + Bu^2)^2, \qquad v' = -v((A + Bu^2)^2 - 2Bv^2). \tag{29}$$

If $AB > 0$ the origin $O' = (0, 0)$ is the unique infinite equilibrium point of system (29) on $v = 0$, and it is an attracting hyperbolic node because its two eigenvalues are all $-A^2$.

If $AB < 0$ system (29) has three equilibria O', $M' = (\sqrt{-A/B}, 0)$ and $N' = (-\sqrt{-A/B}, 0)$ for $v = 0$, where O' is an attracting hyperbolic node, M' and N' are linearly zero. We translate the point M' to the origin doing the change of variables $(u, v) \to (u + \sqrt{-A/B}, v)$, and system (29) becomes

$$\begin{aligned} u' &= -B^2u^2(\sqrt{-A/B} + u)(2\sqrt{-A/B} + u)^2, \\ v' &= -v(B^2u^2(2\sqrt{-A/B} + u)^2 - 2Bv^2). \end{aligned} \tag{30}$$

Applying the blow-up technique and taking into account the behavior of the flow on the axes, i.e. $u'|_{v=0} = 4AB\sqrt{-A/B}u^2 + O(u^3)$ and $v'|_{u=0} = 2Bv^3$, we obtain that the local phase portrait at the origin of system (30) has two hyperbolic sectors and one parabolic sector, as it is shown in Figure 12(a) and 12(b) when $B > 0$ and $B < 0$, respectively.

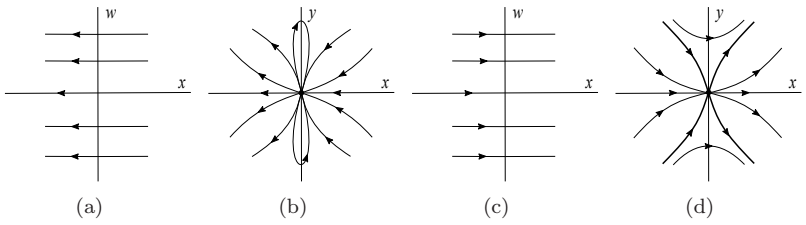

FIGURE 13. Blow-up of the origin of of system (28). (a) System (33) with $B > 0$, (b) System (28) with $B > 0$, (c) System (33) with $B < 0$, (b) System (28) with $B < 0$.

Translating the point N' to the origin doing the change of variables $(u, v) \to (u - \sqrt{-A/B}, v)$, and we obtain the system

$$\begin{aligned} u' =& B^2u^2(\sqrt{-A/B} - u)(2\sqrt{-A/B} - u)^2, \\ v' =& -v(B^2u^2(2\sqrt{-A/B} - u)^2 - 2Bv^2). \end{aligned} \tag{31}$$

Similarly we have that the phase portrait at the origin of system (31) consists of two hyperbolic sectors and one parabolic sector, see Figure 12(c) and 12(d).

In the local chart U_2 system (28) has the form

$$u' = (B + Au^2)^2, \qquad v' = 2Buv^3. \tag{32}$$

Hence the origin of U_2 is not an equilibrium point.

Note that the degree of system (28) is 4, the flow in the charts $V_{1,2}$ have the opposite sense with respect to the sense of the charts $U_{1,2}$, respectively. Thus system (28) has two infinite equilibrium points when $AB > 0$, the equilibrium point O' in U_1 and its diametrically opposite O'' in V_1. But system (28) has six infinite equilibria when $AB < 0$. The equilibrium points O', M' and N' in U_1, and their diametrically opposite O'', M'' and N'' in V_1. On the other hand, the set $L = \{(x, y)|Ax^2 + By^2 = 0\}$ is the origin when $AB > 0$. When $AB < 0$ it is a couple of straight lines $y = \pm\sqrt{-A/B}x$, which connects either the equilibria M' and M'', or N' and N''. Thus the points M', M'', N' and N'' are virtual points of system (27).

Now we focus on the finite equilibrium points for system (28) and for the discontinuous Hamiltonian system (27).

(i.a) If $A > 0$ and $B > 0$, system (28) has three finite equilibrium points $p_1 = (0, 0)$ and $p_{2,3} = (\pm\sqrt{2B}/A, 0)$, where p_1 is linearly zero, p_2 is hyperbolic saddle with the eigenvalues $\lambda_1 = 4\sqrt{2B^3}/A$ and $\lambda_2 = -2\sqrt{2B^3}/A$, and p_3 is hyperbolic saddle with the eigenvalues $\lambda_3 = -4\sqrt{2B^3}/A$ and $\lambda_4 = 2\sqrt{2B^3}/A$. So we need to apply a blow-up $(x, y) \to (x, w)$ with $w = y/x$ for studying the local phase portrait of p_1, and after eliminating the common factor x^2 system (28) becomes

$$x' = -2B + A^2x^2 + 2ABw^2x^2 + B^2w^4x^2, \qquad w' = xw^2(A + Bw^2). \tag{33}$$

System (33) has not equilibria on $x = 0$, thus we consider the local phase portrait in the neighborhood $x = 0$, see Figure 13(a). Going back to system (28) we get

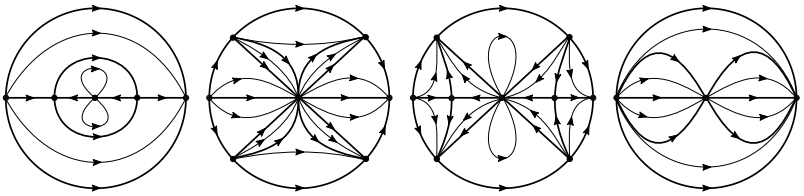

FIGURE 14. The phase portrait of system (28). (a) $A > 0$ and $B > 0$, (b) $A > 0$ and $B < 0$, (c) $A < 0$ and $B > 0$, (d) $A < 0$ and $B < 0$.

that the origin consists of two elliptic sectors and two parabolic sectors, see Figure 13(b). We have that one stable and one unstable separatrices of the saddle p_2 must cross the y-axis and connect with the unstable and the stable separatrices of the saddle p_3. And the energy level $H_3(x, y) = h$ at the saddles $p_{2,3}$ are equal. The other unstable separatrix of the saddle p_2 and the other stable separatrix of the saddle p_3 connect with p_1. Therefore the phase portrait of system (28) is given in Figure 14(a). Going back to the Hamiltonian system (27), the x-axis is filled of equilibrium points and the equilibrium point p_1 of system (28) is a virtual point, because it is in the set L. By the rescaling time $dt = (Ax^2 + By^2)^2 d\tau/y$ the orbits of system (27) have the opposite sense with respect to the ones of system (28) in the region $y < 0$. Hence the phase portrait of system (27) is topologically equivalent to the phase portrait 1.27 of Figure 2.

(i.b) If $A > 0$ and $B < 0$, system (28) has one finite equilibrium point $p_1 = (0, 0)$, which is linearly zero. We apply the blow-up technique and have that the local phase portrait at p_1 consists of two hyperbolic sectors and two parabolic sectors, see Figure 13(d). Using the previous analysis the phase portrait of system (28) is given in Figure 14(b). Going back to system (27), the x-axis is filled of equilibrium points of system (27) and the point p_1 is a virtual point, because it is in the set L corresponding two straight lines $y = \pm\sqrt{-A/B}x$. Similarly system (27) has the opposite sense with respect to the ones of system (28) in the region $y < 0$. Hence the phase portrait of system (27) in this subcase is topologically equivalent to 1.28 of Figure 2.

(i.c) If $A < 0$ and $B > 0$, system (28) has three finite equilibria $p_1 = (0, 0)$ and $p_{2,3} = (\pm\sqrt{2B}/A, 0)$. The equilibria p_1 is linearly zero, whose local phase portrait has two elliptic sectors and two parabolic sectors see Figure 13(b), and $p_{2,3}$ are hyperbolic saddles. Hence the phase portrait of system (28) is shown in Figure 14(c). Similarly to the above cases it is easy to obtain that the phase portrait of system (28) is topologically equivalent to the one of 1.29 in Figure 2.

(i.d) If $A < 0$ and $B < 0$, system (28) has one finite equilibrium point $p_1 = (0, 0)$. The equilibrium point p_1 is linearly zero and its local phase portrait is given in Figure 13(d). Similarly the phase portrait of system (28) is topologically equivalent to the one of Figure 14(d). Therefore we have the phase portrait of the Hamiltonian system (28) is shown in 1.30 of Figure 2.

(ii) Now we consider the case $C \neq 0$, by the rescaling time $dt = (Ax^2 + By^2)^2 d\tau$, system (27) has the form

$$x' = y(Ax^2 + By^2 + C)^2 - 2Bx^2 y, \qquad y' = -2x(C + By^2). \tag{34}$$

From (8) system (34) in U_1 becomes

$$\begin{aligned} u' =& -u^2(A + Bu^2)^2 - 2Cu^2v^2(A + Bu^2) - C(2 + Cu^2)v^4, \\ v' =& -uv((A + Bu^2)^2 - 2(B - AC)v^2 + Cv^2(2Bu^2 + Cv^2)). \end{aligned} \tag{35}$$

If $AB > 0$ system (35) has one equilibrium point $O' = (0, 0)$ in $v = 0$, and it is linearly zero. Using the blow-up technique we have that the local phase portrait at O' consists of two hyperbolic sectors and two parabolic sectors if $C > 0$, see Figure 3(d). And it consists of two elliptic sectors and two parabolic sectors when $C < 0$, as it is shown in Figure 3(c).

If $AB < 0$ system (35) has three equilibrium points O', $M' = (\sqrt{-A/B}, 0)$ and $N' = (-\sqrt{-A/B}, 0)$ when $v = 0$, which are linearly zero. In Figures 3(d) and 3(c), it is shown the local phase portrait of O' when $C > 0$ and $C < 0$, respectively. Doing the changes of variables $(u, v) \to (u + \sqrt{-A/B}, v)$ and $(u, v) \to (u - \sqrt{-A/B}, v)$, we have the systems

$$\begin{aligned} u' =& -B^2u^2(\sqrt{-A/B} + u)(2\sqrt{-A/B} + u)^2 - 2Cv^4 - C^2v^4(\sqrt{-A/B} + u)^2 \\ & - 2BCuv^2(\sqrt{-A/B} + u)^2(2\sqrt{-A/B} + u), \\ v' =& -v(\sqrt{-A/B} + u)(B^2u^2(2\sqrt{-A/B} + u)^2 - 2(B - AC)v^2 + C^2v^4 \\ & + 2BCv^2(\sqrt{-A/B} + u)^2), \end{aligned} \tag{36}$$

and

$$\begin{aligned} u' =& -B^2u^2(\sqrt{-A/B} - u)(2\sqrt{-A/B} - u)^2 - 2Cv^4 - C^2v^4(\sqrt{-A/B} - u)^2 \\ & + 2BCuv^2(\sqrt{-A/B} - u)^2(2\sqrt{-A/B} - u), \\ v' =& v(\sqrt{-A/B} - u)(B^2u^2(2\sqrt{-A/B} - u)^2 - 2(B - AC)v^2 + C^2v^4 \\ & + 2BCv^2(\sqrt{-A/B} - u)^2), \end{aligned} \tag{37}$$

respectively. Then the equilibrium points M' and N' move to the origin. Doing the blow-up technique and taking into account the behavior of the flow on the axes, we obtain that the local phase portrait at the origin of system (36) (or system (37)) has two hyperbolic sectors and one parabolic sector, as it is shown in Figure 12(a) and 12(b) when $B > 0$ and $B < 0$ (or $B < 0$ and $B > 0$), respectively .

In the local chart U_2 system (35) becomes

$$\begin{aligned} u' =& (B + Au^2)^2 + 2C(B + Au^2)v^2 + c(c + 2u^2)v^4, \\ v' =& 2uv^3(B + Cv^2). \end{aligned} \tag{38}$$

Thus the origin is not an equilibrium point in U_2.

Thus the associated polynomial system (35) has two infinite equilibrium points when $AB > 0$, the equilibrium point O' in U_1 and its diametrically opposite O'' in V_1. When $AB < 0$ it has six infinite equilibria, the equilibrium points O', M' and N' in U_1, and their diametrically opposite O'', M'' and N'' in V_1. Note that the degree of system (35) is 5 so the flow in the chart V_1 has the same sense as in U_1.

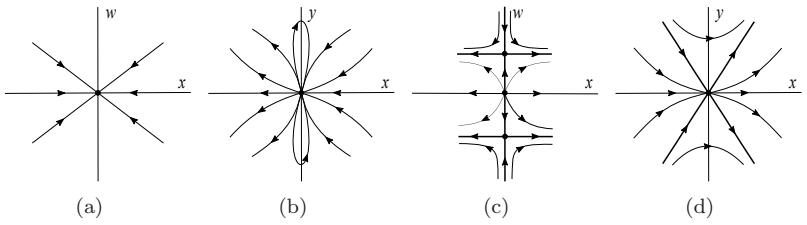

FIGURE 15. Blow-up of the origin of system (39). (a) System (40) with $B > 0$ and $C < 0$, (b) System (39) with $B > 0$ and $C < 0$, (c) System (40) with $B < 0$ and $C > 0$, (b) System (39) with $B < 0$ and $C > 0$.

Now we study the global dynamics of system (27). System (35) has at most seven finite equilibrium points, as the following

$$p_1 = (0, 0), \qquad p_{2,3} = (0, \pm\sqrt{-C/B}),$$
$$p_{4,5} = (\sqrt{2B}/A, \pm\sqrt{-C/B}), \qquad p_{6,7} = (-\sqrt{2B}/A, \pm\sqrt{-C/B}).$$

We will give all the possible phase portraits of system (27) in the Poincaré disk in function of the parameters A, B and C.

(ii.a) Assume that $A > 0$ and $B > 0$. If $C > 0$ system (35) has one finite equilibrium point p_1, which is a center with eigenvalues $\lambda_{1,2} = \pm\sqrt{-2C^3}$. And this system has two infinite equilibria O' and O''. Hence in this subcase the phase portrait of the smooth Hamiltonian system (27) is topologically equivalent to the one shown in 1.8 of Figure 1.

If $C < 0$ system (35) has seven finite equilibrium points p_i $(i = 1, 2, \cdots, 7)$, where $p_{2,3}$ are linearly zero and the other equilibria are hyperbolic saddles with eigenvalues $\lambda_{3,4} = \pm 4B\sqrt{-2C}/A$. By the change of variables $(x, y) \to (x, y + \sqrt{-C/B})$, then the equilibrium point p_2 moves to the origin and system (34) are written in the new variables as

$$\begin{aligned} x' =& (\sqrt{-C/B} + y)(-2Bx^2 + (Ax^2 + By(2\sqrt{-C/B} + y))^2), \\ y' =& -2Bxy(2\sqrt{-C/B} + y). \end{aligned} \tag{39}$$

Applying the directional blow-up $(x, y) \to (u, w)$ with $w = y/x$ and eliminating the common factor x we have

$$\begin{aligned} x' =& x(\sqrt{-C/B} + xw)(-2B + (Ax + Bw(2\sqrt{-C/B} + xw))^2), \\ w' =& -w(B^2w^4x^2(5\sqrt{-C/B} + wx) + Ax(-4Cw + Ax\sqrt{-C/B} + wx)) \\ & + 2B(\sqrt{-C/B} + w^2(Ax^2(3\sqrt{-C/B} + wx) - 2C(\sqrt{-C/B} + 2wx)))). \end{aligned} \tag{40}$$

For $x = 0$ we have $w' = -w(2B\sqrt{-C/B} - 4BC\sqrt{-C/B}w^2)$, thus system (40) has only one equilibrium point $E_1 = (0, 0)$, which is an attracting node with two same eigenvalues $-2B\sqrt{-C/B}$, see Figure 15(a). Going back through the change of variables to system (39) and taking into account the behavior of the flow on the axes, we have $x'|_{y=0} = -2B\sqrt{-C/B}x^2 + O(x^4)$, $x'|_{x=0} = -4BC\sqrt{-C/B}y^2 + O(y^3)$ and $y'|_{x=0} = 0$. Then we obtain the local phase portrait at the origin has two elliptic

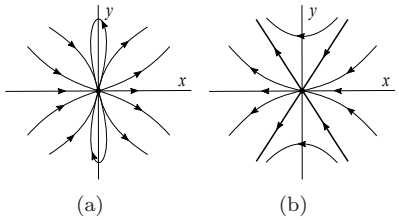

FIGURE 16. Local phase portrait at p_3 of system (28) after moving to the origin. (a) If $C < 0$, (b) If $C > 0$.

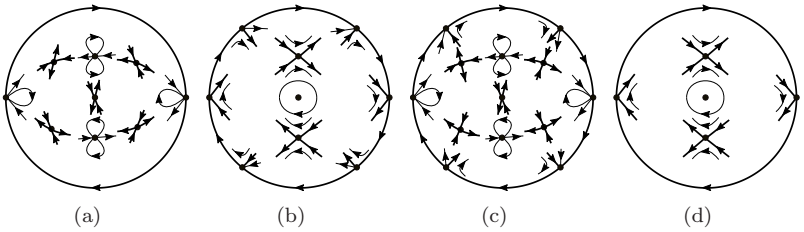

FIGURE 17. Local phase portraits at the equilibrium points of system (35) with $ABC \neq 0$.

sectors and two parabolic sectors, see Figure 15(b). Similarly we obtain that the local phase portrait at p_3 as it is shown in Figure 16(a). The local phase portrait at the equilibrium points of system (35) is shown in Figure 17(a).

One stable separatrix of p_4 must cross the positive x-axis, because it can not intersect the separatrix of itself, to connect with the unstable separatrix of p_5. The other separatrix of p_4 connects with the unstable separatrix of p_6 crossing the y-axis. One unstable separatrix of p_4 connects with p_2. By the symmetries the analogous happens with the separtrices of $p_{5,6,7}$. It is easy to verify that the energy level h of the saddles $p_{4,5,6,7}$ is the same. Going back to the discontinuous Hamiltonian system (27), $p_{2,3}$ are two virtual points because they are in the set $L = \{(x, y)|Ax^2 + By^2 + C = 0\}$, which is an ellipse. Thus the phase portrait of system (27) is topologically equivalent to the one shown in 1.31 of Figure 2.

(ii.b) Assume $A > 0$ and $B < 0$. If $C > 0$ system (35) has three finite equilibrium points $p_{1,2,3}$, where p_1 is a center and $p_{2,3}$ are linearly zero. Similarly to the above case, doing the blow-up we obtain that system (40) has three equilibria $E_1 = (0, 0)$, which is a repelling node, and $E_{2,3} = (0, \pm\sqrt{2C}/(2C))$, which are saddles with eigenvalues $\pm 4B\sqrt{-C/B}$, see Figure 15(c). Going back through the blow-up and taking into account the behavior of the flow on the axes, we have that the local phase portrait at origin of system (39) has two hyperbolic sectors and two parabolic sectors, this is shown in Figure 15(d). In addition we can obtain that the local phase portrait at p_3 has two hyperbolic sectors and two parabolic sectors, see Figure 16(b) (after moving to the origin).

And system (35) has six infinite equilibria O', O'', M', M'', N' and N'', see Figure 17(b). The set L in the Poincaré disk is a hyperbola connecting either the points M' with N'', and N' with M''. Hence they are virtual points. On the other hand $p_{2,3}$ are virtual points because they are in the set L.

If one stable and one unstable separatrices of p_2 connect with the unstable and the stable separatrices of p_3, respectively, then the phase portrait of the Hamiltonian system (27) is topologically equivalent to the one shown in 1.32 of Figure 2. If one stable and one unstable separatrices of p_2 connect with the unstable separatrix of O'' and the unstable separatrix of O' respectively, then the phase portrait of system (27) is topologically equivalent to 1.33 of Figure 2. If one stable and one unstable separatrices of p_2 connect with O'' and O' respectively, and the stable and the unstable separatrices of O'' connect with the unstable and the stable separatrices of O', respectively, then we obtain the phase portrait 1.34 of Figure 2.

On the other hand, if $C < 0$ system (35) has only one finite equilibrium point p_1, and it is a hyperbolic saddle. Thus it is topologically equivalent to the phase portrait 1.11 of Figure 1.

(ii.c) Assume that $A < 0$ and $B > 0$. If $C > 0$ system (35) has one finite equilibrium point p_1, and it is a center, And it has six infinite equilibria O', O'', M', M'', N' and N'', see Figure 6(b). Going back to the rational Hamiltonian system (27), the infinite equilibria M', M'', N' and N'' are virtual points, because the set $L = \{(x, y)|Ax^2 + By^2 + C = 0\}$ in the Poincaré disk is a hyperbola connecting either the points M' with N', and M'' with N''. Thus the phase portrait of the discontinuous Hamiltonian system (27) is topologically equivalent to the one shown in 1.12 of Figure 1.

If $C < 0$ system (35) has seven finite equilibrium points $p_{1,2,\cdots,7}$, where $p_{2,3}$ are linearly zero and the other equilibria are hyperbolic saddles. Similarly to the case (ii.a), the local phase portraits of $p_{2,3}$ have two elliptic sectors and two parabolic sectors see Figures 15(b) and 16(a). And system (35) has six infinite equilibria O', O'', M', M'', N' and N'', their local phase portraits are shown in Figure 17(c). It is check that the energy level h of the saddles $p_{4,5,6,7}$ is the same. Thus the saddles $p_{4,5}$ are connected by one of their separatrices crossing the positive x-axis, and the other separatrix of each one connect with $p_{2,3}$, respectively. By the symmetries the analogous happens with the separtrices of $p_{5,6,7}$. Going back to the rational Hamiltonian system (27), $p_{2,3}$ are two virtual points because they are in the set L, which is a hyperbola connecting either the points M' with N'', and N' with M''. Therefore system (27) has only two infinite equilibrium points. We obtain that the phase portrait is topologically equivalent to 1.35 of Figure 1.

(ii.d) Finally we assume that $A < 0$ and $B < 0$. If $C > 0$ system (35) has three finite equilibrium points $p_{1,2,3}$, where p_1 is a center and $p_{2,3}$ are linearly zero. Similarly to case (ii.a), using the blow-up we obtain that the local phase portraits at $p_{2,3}$ both have two hyperbolic sectors and two parabolic sectors, see Figures 15(d) and 16(b). It is shown in Figure 17(d) the local phase portraits at all equilibrium points of system (35). Going back to system (27) the points $p_{2,3}$ are two virtual points because they are in the set L, which is an ellipse. From the previous information we obtain the phase portrait 1.36 of Figure 2.

If $C < 0$ the system has only one finite equilibrium point p_1, which is a hyperbolic saddle. Therefore we get that the phase portrait is topologically equivalent to 1.1 of Figure 1.

Thus we conclude the proof of Theorem 1.3.

Acknowledgments

The first author is partially supported by National Natural Science Foundation of China (No. 11771059) and China Scholarship Council (No. 201706130102). The second author is partially supported by the Ministerio de Economía, Industria y Competitividad, Agencia Estatal de Investigación grant MTM2016-77278-P (FEDER), the Agència de Gestió d'Ajuts Universitaris i de Recerca grant 2017 SGR 1617, and the European project Dynamics-H2020-MSCA-RISE-2017-777911.

References

[1] M. J. Álvarez, A. Ferragut, X. Jarque, A survey on the blow up technique, Int. J. Bifurcation Chaos 31, (2011) 3103–3118.
[2] J. Artés, J. Llibre, Quadratic Hamiltonian vector fields, J. Differential Equations 107 (1994) 80–95.
[3] T. R. Blows, C. Rousseau, Bifurcation at infinity in polynomial vector fields, J. Differential Equations 104 (1993) 215–242.
[4] F. Cao, J. Jiang, The Classification on the Global Phase Portraits of Two-dimensional Lotka-Volterra System, J. Dynam. Differential Equations 20 (2008) 797–830.
[5] H. Chen, X. Chen, Dynamical analysis of a cubic Liénard system with global parameters, Nonlinearity 28 (2015) 3535–3562.
[6] H. Chen, X. Chen, Dynamical analysis of a cubic Liénard system with global parameters (II), Nonlinearity 29 (2016) 1798–1826.
[7] H. Chen, X. Chen, J. Xie, Global phase portrait of a degenerate Bogdanov-Takens system with symmetry, Discrete Contin. Dyn. Syst. Ser. B 22 (2017) 1273–1293.
[8] H. Chen, J. Llibre, Y. Tang, Global dynamics of a SD oscillator, Nonlinear Dyn. 91 (2018) 1755–1777.
[9] T. Chen, L. Huang, P. Yu, W. Huang, Bifurcation of limit cycles at infinity in piecewise polynomial systems, Nonlinear Anal.: Real World Appl. 41 (2018) 82–106.
[10] I. Colak, J. Llibre, C. Valls, Hamiltonian linear type centers of linear plus cubic homogeneous polynomial vector fields, J. Differential Equations 257 (2014) 1623–1661.
[11] I. Colak, J. Llibre, C. Valls, Hamiltonian nilpotent centers of linear plus cubic homogeneous polynomial vector fields, Adv. Math. 259 (2014) 655–687.
[12] I. Colak, J. Llibre, C. Valls, Bifurcation diagrams for Hamiltonian linear type centers of linear plus cubic homogeneous polynomial vector fields, J. Differential Equations 258 (2015) 846–879.
[13] I. Colak, J. Llibre, C. Valls, Bifurcation diagrams for Hamiltonian nilpotent centers of linear plus cubic homogeneous polynomial vector fields, J. Differential Equations 262 (2017) 5518–5533.
[14] F. Dumortier, J. Llibre, J. Artés, Qualitative Theory of Planar Differential Systems, Universitext, Springer-Verlag, New York, 2006.
[15] A. Gasull, A. Guillamon, V. Mañosa, Phase portrait of Hamiltonian systems with homogeneous nonlinearities, Nonlinear Anal. 42 (2000) 679–707.
[16] A. Guillamon, C. Pantazi, Phase portraits of separable Hamiltonian systems, Nonlinear Anal. 74 (2011) 4012–4035.
[17] H. Liang, J. Huang, L. Zhao, Classification of global phase portraits of planar quartic quasi-homogeneous polynomial differential systems, Nonlinear Dyn. 78 (2014) 1659–1681.
[18] J. Llibre, Y. Martínez, C. Vidal, Linear type centers of polynomial Hamiltonian systems with nonlinearities of degree 4 symmetric with respect ot the y-axis, Discrete Contin. Dyn. Syst. Ser. B 23 (2018) 997–912.

[19] J. Llibre, R. D. S. Oliveira, Phase portraits of quadratic polynomial vector fields having a rational first integral of degree 3, Nonlinear Anal. 70 (2009) 3549–3560.
[20] L. Markus, Global structure of ordinary differential equations in the plane, Trans. Amer. Math. Soc. 76 (1954) 127–148.
[21] Y. Martínez, C. Vidal, Classification of global phase portraits and bifurcation diagrams of Hamiltonian systems with rational potential, J. Differential Equations 261 (2016) 5923–5948.
[22] D. Neumann, Classification of continuous flows on 2-manifolds, Proc. Amer. Math. Soc. 48 (1975) 73–81.
[23] M. Peixoto, Dynamical Systems, Proceedingsof a Symposium held at the University of Bahia, Acad. Press, New York, 1973, pp.389–420.
[24] D. Schlomiuk, Algebraic particular integrals, integrability and the problem of the center, Trans. Amer. Math. Soc. 338 (1993) 799–841.
[25] N. Vulpe, Affine-invariant conditions for topological distinction of quadratic systems in the presence of a center (Russian), Differ. Equ. 19 (1983) 371–379.

[1] College of Mathematics and Econometrics, Hunan University, Changsha, 410082, PR China

E-mail address: chenting0715@126.com

[2] Departament de Matemàtiques, Universitat Autònoma de Barcelona, 08193 Bellaterra, Barcelona, Catalonia, Spain

E-mail address: jllibre@mat.uab.cat

*Corresponding author